JOURNAL OF MATERIALS SCIENCE 28 (1993) 6657–6664

Selective, low-temperature synthesis of niobium carbide and a mixed (niobium/tungsten) carbide from metal oxide–polyacrylonitrile composites by carbothermal reduction

B. F. DAL, S. G. HARDIN, D. G. HAY, T. W. TURNEY
CSIRO Division of Materials Science and Technology, Locked Bag 33, Clayton 3168, Victoria, Australia

Composites of polyacrylonitrile (PAN) with the layered oxides $(C_6H_{13}NH_3)Nb_3O_8$, $(C_8H_{17}NH_3)Nb_3O_8$ and α-$(C_6H_{13}NH_3)NbWO_6$ undergo carbothermal reduction in an argon atmosphere at 1000 °C to give the cubic carbides NbC_x and (Nb, W)C_x, respectively. Reduction of the Nb_3O_8/PAN composites to NbC_x proceeds via the formation of tetragonal NbO_2, with no other intermediates being detected. Formation of NbC_x begins at 800 °C but is not complete until 1000 °C. The resultant carbide appears in a highly porous form in admixture with approximately 50% wt/wt amorphous carbon. The carbide content, x, of cubic NbC_x increases with heating time (at 1000 °C) as expected. Values of x ranging from 0.69–0.95 have been observed. The cubic mixed carbide, (Nb, W)C_x, is formed similarly from the α-$NbWO_6$ system via an alkylammonium form in the presence of PAN, although progressive separation into cubic NbC_x and hexagonal WC_x occurs at temperatures above 1000 °C. The β-$NbWO_6$ system does not form a well-defined alkylammonium salt; instead a mixture of β-$HNbWO_6$ with PAN gives rise to a very poorly crystalline (Nb, W) carbide on reduction. In all cases, both a layered oxide and PAN are necessary to form the pure carbides at 1000 °C. The oxide/PAN composites appear to be intimate physical mixtures rather than ordered layered nanocomposites.

1. Introduction

The monocarbides of niobium and tungsten are of commercial importance as the principal components in cemented carbide cutting tools and abrasives [1]. Conventional synthesis of WC is from pure tungsten powder and carbon black at 1400–1600 °C, whilst NbC is made from Nb_2O_5 and carbon at 1600–1800 °C [1]. Niobium and tungsten form a cubic mixed carbide, (Nb, W)C_x, which is also commercially important [1]. Recently, β′-sialons, silicon carbide and aluminium nitride have been prepared at relatively low temperatures from layered aluminosilicates containing intercalated organics [2, 3]. Heat treatment of these in nitrogen gives rise to ordered oxide–carbon layered nanocomposites, which in a subsequent carbothermal reduction, form the ceramics with high selectivity [4, 5], and at lower temperatures than those used in conventional preparations.

Extension of this technique to the production of transition metal carbides such as those of tungsten and niobium was thus thought feasible. Suitable layered precursors for composite formation are KNb_3O_8, with an orthorhombic structure [6], and α-$LiNbWO_6$, with a tetragonal trirutile structure [7]. Both materials contain readily exchangeable alkali metal cations in the interlayer region [8–10], and the layered structures are preserved in the proton forms after acid exchange in nitric acid [11, 12]. In addition, both HNb_3O_8 and α-$HNbWO_6$, as solid-state Brönsted acids, have been shown to undergo layer expansion following intercalation of long-chain amines [12, 13]. β-$LiNbWO_6$, with the hexagonal (rhombohedral) $LiNbO_3$ structure [8, 14], is acid-exchanged in refluxing 9M H_2SO_4 to give β-$HNbWO_6$ [15].

This paper discusses the preparation and carbothermal reduction of alkylammonium Nb_3O_8/PAN composites. In addition, the analogous reactions involving the α- and β-$NbWO_6$ systems are compared.

2. Experimental procedure

2.1. Materials

Potassium nitrate (AR), nitric acid (AR), sulphuric acid (AR), acrylonitrile (LR), benzoyl peroxide (Tech) and toluene (AR) were obtained from Ajax Chemicals, lithium carbonate (LR), tungsten oxide (LR) and light petroleum spirit (b.p. range 40–60 °C) from BDH

0022–2461

Chemicals, niobium oxide (99.9%) and 1-amino-octane (97%) from Aldrich Chemicals Inc, heptane (99%) from Waters Associates, 1-aminohexane (99%) from Fluka Chemicals, and high-purity graphite powder (1–2 μm particle size) from Acheson Pty Ltd.

2.2. Intermediates

KNb_3O_8 was prepared by a reported method [11] from KNO_3 and Nb_2O_5. α-$LiNbWO_6$ was prepared from Li_2CO_3, WO_3 and Nb_2O_5 powders (used as-supplied). The starting materials (equimolar in lithium, niobium and tungsten) were placed in a polypropylene container containing several polyacrylic balls to assist blending, and mixed using a mechanical shaker for 45 min. The resultant mixture was compressed into pellets of approximately 2 cm diameter and fired in air at 750–760 °C for 144 h. The white product was ground to a fine powder prior to use. β-$LiNbWO_6$ was prepared similarly to the α-form, but fired at 800–840 °C for 2–4 h only. $HNb_3O_8 \cdot H_2O$ was prepared from KNb_3O_8 (10 g) by exchange in 7M nitric acid (1 l) at room temperature with stirring for 72 h [11], while α-$HNbWO_6 \cdot 1.5H_2O$ was prepared from α-$LiNbWO_6$ (4 g) by exchange in refluxing 6M nitric acid (250 cm^3) with stirring for 24 h [12], and β-$HNbWO_6$ was prepared from β-$LiNbWO_6$ (4 g) by exchange in refluxing 9M sulphuric acid (150 cm^3) with stirring for 24 h [15].

$(C_8H_{17}NH_3)Nb_3O_8$ was prepared by a variation of the literature method [13]. $HNb_3O_8 \cdot H_2O$ (3 g) was suspended in a solution of 1-amino-octane (15 cm^3) in heptane (135 cm^3), and the mixture refluxed with stirring for 24 h. After cooling, the product was separated by filtration, washed with heptane (3×100 cm^3) and air-dried overnight at room temperature. $(C_6H_{13}NH_3)Nb_3O_8$ was prepared similarly, using 1-aminohexane [13]. α-$(C_6H_{13}NH_3)NbWO_6$ was prepared from α-$HNbWO_6 \cdot 1.5H_2O$ and 1-aminohexane in a similar manner to the above [12].

Polyacrylonitrile powder (PAN) was prepared from a mixture of acrylonitrile (50 cm^3), toluene (450 cm^3) and benzoyl peroxide (0.5 g) by refluxing with stirring for 24 h, cooling and filtering. The pale-yellow powder was washed with toluene (3×200 cm^3) and light petroleum (3×200 cm^3) then air-dried at room temperature overnight.

$(C_8H_{17}NH_3)Nb_3O_8$/PAN composite (1a): $(C_8H_{17}NH_3)Nb_3O_8$ (3 g) was suspended in a solution of benzoyl peroxide (0.2 g) and acrylonitrile (20 cm^3) in toluene (180 cm^3). The mixture was refluxed with stirring for 24 h, cooled and filtered. The product was washed with toluene (3×100 cm^3) then light petroleum (3×100 cm^3) and air-dried at room temperature overnight. Prior to heating, the pale-yellow powder was pressed into cylindrical tablets (~ 3 g each, 19 mm diameter, 10 mm length).

The $(C_6H_{13}NH_3)Nb_3O_8$/PAN composite (1b) and the α-$(C_6H_{13}NH_3)NbWO_6$/PAN composite (3) were prepared similarly.

Amorphous carbon from PAN: PAN powder (3 g) was compressed into tablets as above and then heated in an argon atmosphere at 1000 °C/4 h (see heating procedure below). The resultant black tablets were ground to a fine powder in an agate mortar before use.

Niobium oxide phase/carbon source (physical mixtures): the niobium oxide phase (Nb_2O_5 or Nb_3O_8 phase) (0.5 g) and carbon source (graphite, amorphous carbon or PAN) (2.0 g) were ground together thoroughly in an agate mortar. The resultant powder was tabletted as above prior to heating.

2.3. Heating procedure

Samples (~ 3 g each) were heated in graphite boats in a tube furnace fitted with an argon flow system (500 $cm^3\ min^{-1}$, approximate linear velocity 10 $cm\ min^{-1}$). Samples heated at temperatures up to 1000 °C were ramped at 500 °C h^{-1} to the final temperature, whilst those heated to higher temperatures were ramped at 200 °C h^{-1}. They were then held for the appropriate period of time before cooling to ambient in an argon atmosphere.

2.4. Characterization

Powder X-ray diffraction (XRD) data were obtained with a Siemens D-500 Diffractometer (nickel-filtered CuK_α radiation, scan step 0.04°). Patterns were measured from bulk powders for all samples. In addition, dried, oriented films on glass slides were used for selected samples in order to obtain accurate basal spacings. Transmission electron microscopy (TEM) was carried out with a Jeol JEM-100CX electron microscope. Samples were dispersed in alcohol and examined against a holey carbon background.

3. Results and discussion

3.1. Nb_3O_8 system

Table I shows the phases observed by XRD for various reaction mixtures after heating at 1000 °C in an argon atmosphere for 4 h. Table II gives XRD data for key intermediates in the Nb_3O_8 system. The *d* spacings observed for the K^+, H^+, $(C_6H_{13}NH_3)^+$ and $(C_8H_{17}NH_3)^+$ forms are in accord with those in the literature [11, 13, 14]. In particular, the spacings obtained for the alkylammonium forms correspond to those of the anhydrous forms [13]. Slight (0.1–0.2 nm) increases in basal spacing occurred after the attempted intercalation of PAN, but the changes were not sufficient to unequivocally indicate the presence of interlayer PAN.

For reaction mixtures containing both an alkylammonium niobate, $(RNH_3)Nb_3O_8$, and PAN, only the cubic carbide, NbC_x [14], and the tetragonal dioxide, NbO_2 [14], were present after reduction. A 90% yield of carbide was obtained (after 4 h), regardless of whether attempted intercalates (1a or 1b) or physical mixtures (2a or 2b) were used. Furthermore, no difference in reduction behaviour was seen between hexyl- and octylammonium niobates. With longer heating times, complete conversion to the carbide was obtained (see below).

Fig. 1 is a low-resolution transmission electron micrograph of 1b, the unfired $(C_6H_{13}NH_3)Nb_3O_8$/PAN

TABLE I Carbothermal reduction products of niobium oxide phases

Reactants [a]	Products [b]
Nb_2O_5 + graphite	Nb_2O_5(M), graphite
Nb_2O_5 + PAN	20% NbC_x, 80% NbO_2 (T)
Nb_2O_5 + amorphous C (ex PAN)	NbO_2 (M)
$(C_6H_{13}NH_3)Nb_3O_8$	NbO_2(M), Nb_2O_5(M), $Nb_{12}O_{29}$(O)
$(C_8H_{17}NH_3)Nb_3O_8$	NbO_2(M), Nb_2O_5(M), $Nb_{12}O_{29}$(O)
$(C_8H_{17}NH_3)Nb_3O_8$ (preheated at 1000 °C/4 h) + amorphous C (ex PAN)	NbO_2(M), Nb_2O_5(M), $Nb_{11}O_{29}$(O)
$(C_8H_{17}NH_3)Nb_3O_8$ (preheated at 1000 °C/4 h) + PAN	20% NbC_x, 80% NbO_2 (T)
$(C_8H_{17}NH_3)Nb_3O_8$ + amorphous C (ex PAN)	NbO_2(M), $Nb_{12}O_{29}$(M)
$(C_8H_{17}NH_3)Nb_3O_8$/PAN (attempted intercalate, 1a)	90% NbC_x, 10% NbO_2 (T)
$(C_8H_{17}NH_3)Nb_3O_8$ + PAN (physical mixture, 2a)	90% NbC_x, 10% NbO_2 (T)
$(C_6H_{13}NH_3)Nb_3O_8$/PAN (attempted intercalate, 1b)	90% NbC_x, 10%NbO_2 (T)
$(C_6H_{13}NH_3)Nb_3O_8$ + PAN (physical mixture, 2b)	90% NbC_x, 10%NbO_2 (T)

[a] All reactions at 1000 °C for 4 h.
[b] Percentages estimated from ratios of peak heights of 100% peaks with an accuracy of approximately ± 10%. Letters in brackets denote crystal forms (M = monoclinic, T = tetragonal, O = orthorhombic).

TABLE II Experimental XRD data for Nb_3O_8 phases

Phase	d^a_{020} (nm)
KNb_3O_8	1.053 (3)
$(H_3O)Nb_3O_8$	1.113 (3)
$(C_6H_{13}NH_3)Nb_3O_8$	2.235 (6)
$(C_8H_{17}NH_3)Nb_3O_8$	2.426 (6)
$(C_8H_{17}NH_3)Nb_3O_8$/PAN (1a)	2.649 (6)
$(C_6H_{13}NH_3)Nb_3O_8$/PAN (1b)	2.344 (6)

[a] Estimated standard deviation ($\times 10^{-3}$) shown in brackets.

composite. Two phases are clearly visible: (a) large irregular platelets, 0.5–1 μm in size, assigned as $(C_6H_{13}NH_3)Nb_3O_8$. The presence of interlayer PAN is uncertain; (b) fine, poorly structured particles around 0.1 μm or less in size, most likely free PAN. Fig. 2 is a higher resolution transmission electron micrograph of the platelet phase in 1b. Overlapping sheets at the platelet edge are visible. A considerable degree of layer curvature and disorder in stacking is evident, with some lattice fringes visible within the individual sheets. Small, thin aggregates (10–20 nm in size) of a second phase (probably PAN) of poorly-defined morphology are visible near, and possibly between the sheets. Fig. 3 is a similar high-resolution transmission electron micrograph of 1a, the $(C_8H_{17}NH_3)Nb_3O_8$/PAN composite. A selected-area diffraction (SAD) pattern of the platelet phase is

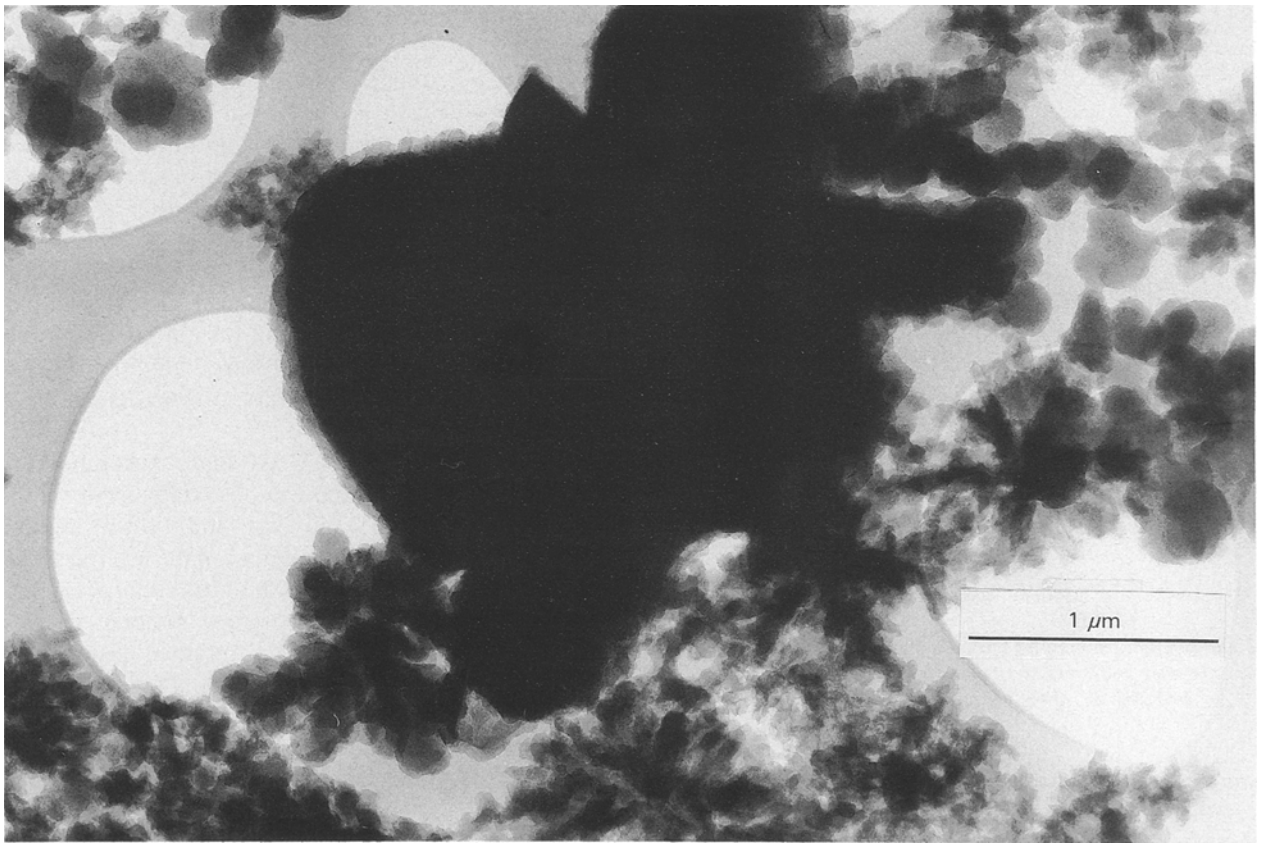

Figure 1 Low-resolution transmission electron micrograph of the unfired $(C_6H_{13}NH_3)Nb_3O_8$/PAN composite (1b).

Figure 2 High-resolution transmission electron micrograph of the unfired $(C_6H_{13}NH_3)Nb_3O_8$/PAN composite (1b).

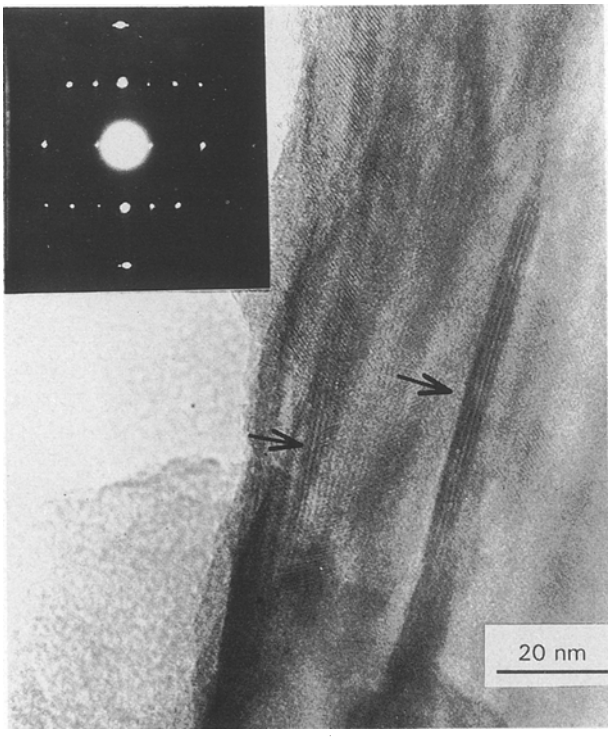

Figure 3 High-resolution transmission electron micrograph (with selected-area diffraction pattern inset) of the unfired $(C_8H_{17}NH_3)Nb_3O_8$/PAN composite (1a).

included. Weak fringes due to the Nb–O octahedra (~ 0.4 nm) are displayed by the majority of the sample, although occasional layer fringes (arrowed) can be seen. Layering of this phase was always ordered over only a few nanometres. Weakly diffracting material (PAN) is visible near the platelet edges.

Fig. 4 is a low-resolution transmission electron micrograph of 1b after reduction for 4 h. The original 1 μm platelets have transformed into highly porous aggregates of NbC_x particles (around 30 nm in size). These are surrounded (and in some cases coated) by amorphous carbon derived from PAN. Large numbers of void spaces are visible within the aggregate. A high-resolution transmission electron micrograph of 1a after reduction for 4 h is shown in Fig. 5. Once again, strongly diffracting crystallites of cubic NbC_x around 30 nm in size (labelled A) are seen. These display lattice fringes 0.26 nm apart, characteristic of d_{111} in these materials [14], in turn implying a cubic unit cell of around 0.45 nm. Large amounts of filamentous or possibly turbostratic carbon derived from PAN are present (B).

In the absence of PAN, hexyl- and octylammonium niobates yielded a mixture of oxides: monoclinic NbO_2, monoclinic Nb_2O_5 and orthorhombic $Nb_{12}O_{29}$ [14]. Complete collapse of the layered structures had occurred, without the formation of carbide phases. Clearly, very little organic material derived from the RNH_3^+ groups was retained at elevated temperatures. Likewise, when the alkylammonium niobates were heated with amorphous carbon (derived from preheated PAN), a mixture of niobium oxides [14] was obtained, indicating that free carbon was insufficiently reactive at 1000 °C to reduce the Nb–O phases. Moreover, when non-layered niobium oxides (either preheated alkylammonium niobates or pure

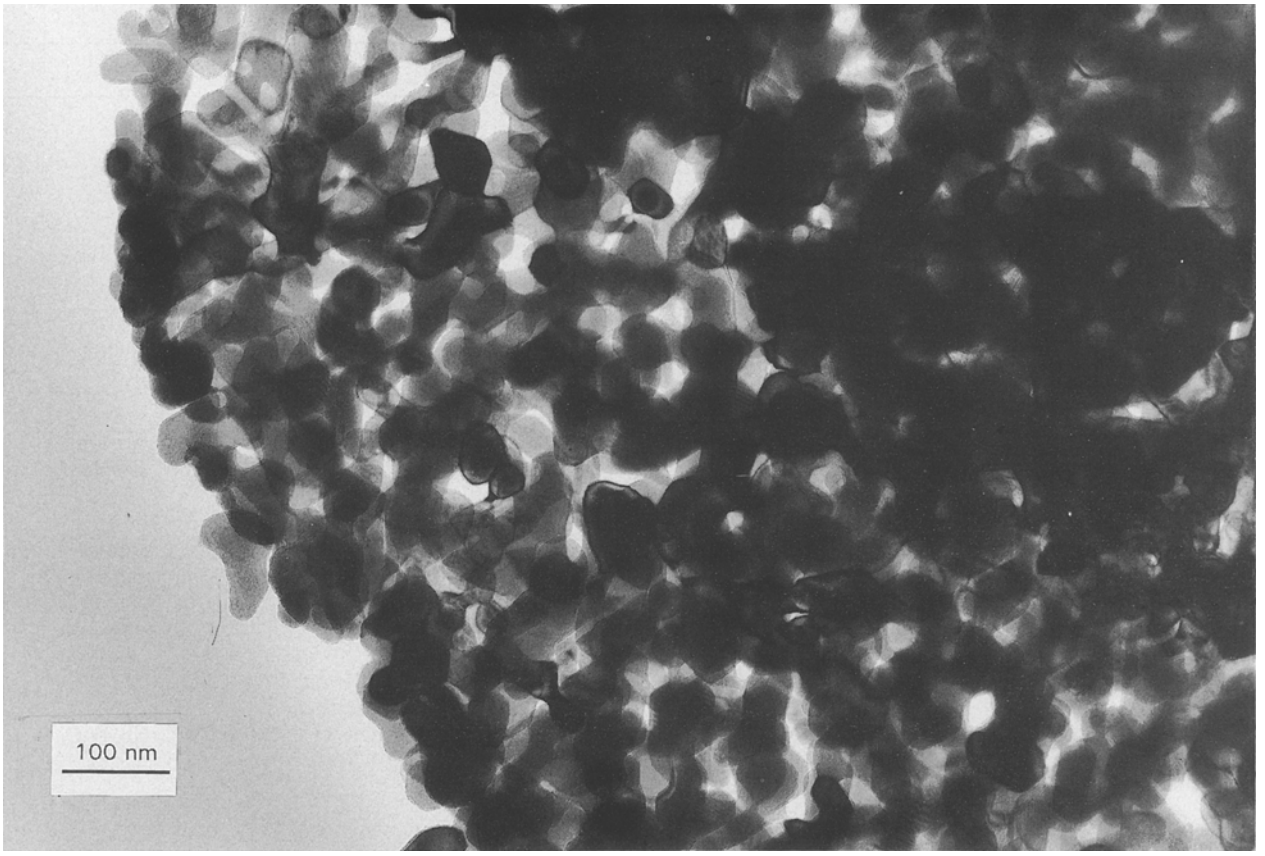

Figure 4 Low-resolution transmission electron micrograph of the $(C_6H_{13}NH_3)Nb_3O_8$/PAN composite (1b) after heating in argon at 1000 °C for 4 h.

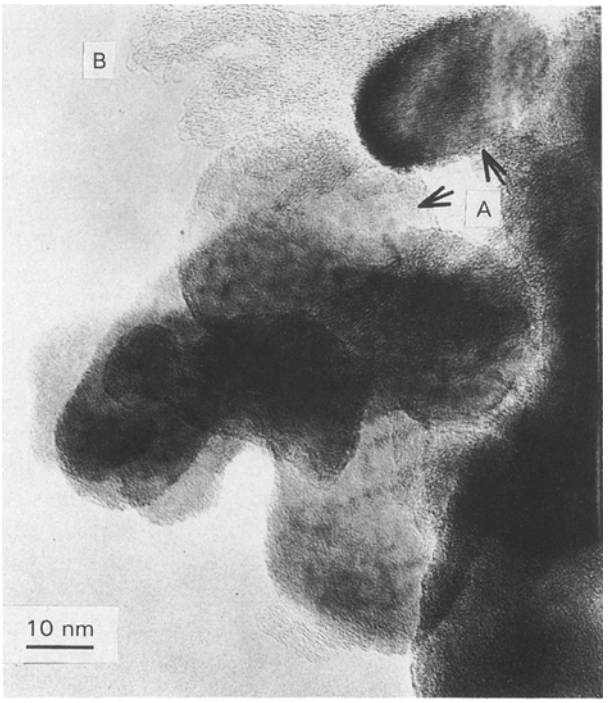

Figure 5 High-resolution transmission electron micrograph of the $(C_8H_{17}NH_3)Nb_3O_8$/PAN composite (1a) after heating in argon at 1000 °C for 4 h.

Nb_2O_5) were used, in admixture either with PAN, amorphous carbon (from PAN at 1000 °C) or crystalline graphite (1–2 μm powder), incomplete reduction occurred. Of the three carbon sources, only PAN resulted in some NbC_x (20% yield), with tetragonal NbO_2 (80% yield) the only other phase detected. When amorphous carbon or graphite was used, a mixture of oxides [14] resulted. In each case, the behaviour of pre-pyrolysed $(C_8H_{17}NH_3)Nb_3O_8$ paralleled that of Nb_2O_5.

Table III compares the phases formed on heating 1a and 2a at various temperatures for 4 h in argon. In both cases, the basal spacing had nearly disappeared by 500 °C, although a weak spacing at 2.37 nm was still observable in the product from 1a. At 700 °C, both materials remained largely amorphous, although very weak peaks due to tetragonal NbO_2 were seen in 2a, together with trace amounts of unidentified phases. At 800 °C, the onset of cubic NbC_x formation for both samples was noted, although only trace amounts were present. The predominant phase, however, for both 1a and 2a at this point was tetragonal NbO_2, with a higher crystallinity in 1a, possibly due to a more even distribution of PAN in the unfired precursor. No other Nb–O phases were detected. By 900 °C, poorly crystalline NbC_x accounted for 60%–70% of the product for both samples. Carbide formation was approximately 90% complete for both samples by 1000 °C, with the remainder being NbO_2. Evidence for the presence of a true metal oxide–PAN intercalate in 1a on the basis of the above product distribution is thus lacking, because any minor differences in behaviour between 1a and 2a on heating can also be rationalized in terms of the degree of niobate–PAN mixing.

TABLE III Reaction products for $(C_8H_{17}NH_3)Nb_3O_8$/PAN (1a) and $(C_8H_{17}NH_3)Nb_3O_8$ + PAN (2a)[a]

Reaction temp. (°C)	$(C_8H_{17}NH_3)Nb_3O_8$/PAN (1a)	$(C_8H_{17}NH_3)Nb_3O_8$ + PAN (2a)
500[b]	Nearly amorphous $d_{(020)}$ = 2.367 (5) nm (vw)	Amorphous
700	Nearly amorphous $d \approx 3.5$ nm (vw, br)	Trace NbO_2(T)
800	NbO_2(T), trace NbC_x	NbO_2 (T), trace NbC_x
900	40% NbO_2 (T), 60% NbC_x	30% NbO_2 (T), 70% NbC_x
1000	10% NbO_2 (T), 90% NbC_x	10% NbO_2 (T), 90% NbC_x

[a] Reaction time 4 h unless stated otherwise.
[b] Reaction time 1 h.

TABLE IV Product composition versus reaction time for $(C_8H_{17}NH_3)Nb_3O_8$/PAN (1a)[a]

Reaction time (h)	NbC_x unit cell a (nm)[b]	Carbide content, x (in NbC_x)[c]	Other phases
0.5	0.4430 (1)	0.69 (1)	30% NbO_2 (T)
0.7	0.4429 (3)	0.69 (1)	30% NbO_2 (T)
1.0	0.4431 (3)	0.70 (1)	25% NbO_2 (T)
1.5	0.4441 (2)	0.74 (1)	20% NbO_2 (T)
2.0	0.4461 (3)	0.86 (3)	10% NbO_2 (T)
4.0	0.4456 (2)	0.83 (2)	10% NbO_2 (T)
8.0	0.4465 (1)	0.90 (1)	Trace NbO_2 (T)
16.0	0.4468 (1)	0.94 (1)	None
48.0	0.4469 (1)	0.95 (2)	None

[a] All reactions at 1000 °C.
[b] Estimated standard deviation ($\times 10^{-4}$) shown in brackets.
[c] Estimated standard deviation ($\times 10^{-2}$) shown in brackets. Variation in x from duplicate experiments is approximately $\pm$ 0.03.

TABLE V Experimental XRD data for α-$NbWO_6$ and β-$NbWO_6$ phases

	Phase	d spacing (nm)[a]
α-$NbWO_6$	$LiNbWO_6$	$d_{(001)}$ = 0.910 (2)
	$HNbWO_6 \cdot 1.5H_2O$	$d_{(002)}$ = 1.283 (4)
	$(C_6H_{13}NH_3)NbWO_6$	$d_{(001)}$ = 2.445 (6)
	$(C_6H_{13}NH_3)NbWO_6$/PAN (attempted intercalate, 3)	$d_{(001)}$ = 2.374 (6)
	$(C_6H_{13}NH_3)NbWO_6$/PAN (3) (Δ 1000 °C/4 h)	Cubic (Nb, W)C_x a = 0.4365 (8)
β-$NbWO_6$	$LiNbWO_6$	$d_{(012)}$ = 0.372 (2)
	$HNbWO_6$	$d_{(200)}$ = 0.377 (2)
	$HNbWO_6 + C_8H_{17}NH_2$ attempted reaction	d = 0.377 (2) (mainly unchanged $HNbWO_6$)
	$HNbWO_6$ + PAN (Δ 1000 °C/4 h)	Cubic (Nb, W)C_x (very poorly crystalline)

[a] Estimated standard deviation in last decimal place shown in brackets.

Table IV gives the unit cell dimension, a, and the composition, x, of the cubic system NbC_x as a function of firing time for 1a at 1000 °C. Values for the unit cell dimension, a, were determined by least-squares fit of five observed and calculated spacings. Values of x were then determined using the relationship to a which has been reported [16] to be of the form

$$10a\ (\text{nm}) = 4.0987 + 0.718\,20x - 0.345\,70x^2 \quad (1)$$

or in terms of x

$$x = 1.0388 - 1.7008\,[4.4715 - 10a(\text{nm})]^{1/2} \quad (2)$$

The value of x in NbC_x generally rose with increasing heating time, from 0.69 (for 0.5 h) to 0.95 (for 48 h), although some scatter in x was observed in the mid-range experiments (2–8 h). The lowest x value observed (0.69) is close to the lower composition limit for the cubic NbC_x system [16]. For shorter firing times, poor carbide crystallinity and resultant broadening of XRD peaks increased the uncertainty in determination of x. Reaction times in excess of 8 h were required to remove all traces of tetragonal NbO_2. After prolonged firing times, the carbide content approached the theoretical interstitial limit.

3.2. α- and β-$NbWO_6$ systems

Table V gives XRD data for various intermediates in the α-$NbWO_6$ system. The parameters observed were in agreement with previously reported values [12, 14, 15]. After attempted intercalation of PAN into α-$(C_6H_{13}NH_3)NbWO_6$ to give α-$(C_6H_{13}NH_3)$-$NbWO_6$/PAN (3), no increase in basal spacing was observed. Composite 3 underwent carbothermal reduction to a cubic mixed carbide (Nb, W)C_x after 4 h at 1000 °C, in a similar manner to the Nb_3O_8 system, with no Nb/W oxide phases being detected after reaction. Table VI summarizes the properties of the carbide phases formed from composite 3 under various conditions of firing. Only a poorly crystalline cubic mixed phase (Nb, W)C_x was seen at 1000 °C, regardless of firing time. At 1200 °C, crystallinity was improved, as evinced by sharper XRD peaks. The unit cell dimension, a, for the cubic mixed carbide was smaller than that of the parent NbC_x lattice, as had been observed by other workers [17]. Separation of hexagonal WC (about 5%) had also begun at this temperature. The trend had become extreme by 1400 °C, when an approximately equimolar mixture of a cubic phase (probably mainly NbC_x with only traces of (Nb, W)C_x) and a hexagonal phase (WC) was observed, implying that separation into component carbides was nearly complete. Assuming the cubic phase in the 1400 °C sample to be NbC_x, the observed a value gives a carbide content of x = 0.76.

The behaviour of the β system differed somewhat from that of the α system. Diffraction data (Table V) for hexagonal β-$LiNbWO_6$ agreed with previously

TABLE VI Carbide phases formed from α-$(C_6H_{13}NH_3)NbWO_6$/PAN (3)

Reaction time (h)	Reaction temp. (°C)	Product (s) and unit cell, a (nm)[a]
4	1000	Poorly crystalline cubic (Nb, W)C_x, $a = 0.4365$ (8)
28	1000	Poorly crystalline cubic (Nb, W)C_x, $a = 0.4365$ (15)
24	1200	95% cubic (Nb, W)C_x, $a = 0.4411$ (13) 5% hexagonal WC
24	1400	50% cubic NbC_x, $a = 0.4448$ (9) 50% hexagonal WC

[a] Estimated standard deviation ($\times 10^{-4}$) shown in brackets.

published values [8, 14, 15], characteristic of the $LiNbO_3$-type structure. On acid exchange in refluxing 9M H_2SO_4, cubic β-$HNbWO_6$ [15] was formed, together with small amounts of unidentified impurities; the latter may have included WO_3 and Nb_2O_5 polytypes or mixed Nb/W oxides formed by dehydration of β-$HNbWO_6$ under the relatively severe exchange conditions. Attempts to produce pure β-$HNbWO_6$ under milder conditions (refluxing 7M HNO_3) resulted in a low degree of proton exchange. β-$HNbWO_6$ showed no tendency to react with 1-amino-octane; no change in basal spacing was observed. Heating an intimate physical mixture of β-$HNbWO_6$ and PAN led, however, to a very poorly crystalline cubic phase, most likely the mixed carbide. Owing to the poor crystallinity, accurate determination of the a value was not possible.

4. Conclusions

From the above results on the carbothermal reduction of the Nb_3O_8 system it appears that the presence of both a layered system and PAN is necessary to achieve selective synthesis of cubic NbC_x at low temperatures (1000 °C). In the absence of PAN, $(RNH_3)Nb_3O_8$ systems undergo irreversible layer collapse to give a mixture of oxides, accompanied by evolution of organics derived from the alkylammonium group. Once formed, these oxides do not undergo reduction to the carbide completely at 1000 °C, regardless of the subsequent carbon source (PAN, amorphous carbon or graphite).

When PAN is present from the beginning of the heating process, however, diffusion of volatile organic pyrolysis products derived from the PAN into the Nb_3O_8 interlayer regions is postulated to occur before layer-collapse. This would then lead to a transient niobium oxide/organic nanocomposite which undergoes facile reduction to the carbide, via tetragonal NbO_2 as an intermediate. If, however, an involatile form of carbon is present rather than PAN in admixture with the layered niobate, diffusion of carbon between the layers cannot occur before the temperatures needed for layer collapse (~ 500 °C), so that Nb_2O_5 results, with subsequent incomplete reduction to a mixture of oxides.

The presence of an ordered nanocomposite in the $(RNH_3)Nb_3O_8$/PAN series at room temperature is doubtful on the basis of (a) the lack of a significant basal spacing increase on attempted intercalation of PAN, and (b) the similar reaction paths of niobate/PAN attempted intercalates and niobate/PAN physical mixtures. However, TEM evidence for the attempted intercalates shows PAN in very close proximity to niobate layers on a nanometre level, so that diffusion of organic material into the interlayer region at elevated temperatures is not surprising. The failure of the Nb_3O_8/α-$NbWO_6$ system to exhibit swelling behaviour with neutral organics (such as acrylonitrile monomer or PAN) can be rationalized in terms of the high layer charge density present in this structure, causing a relatively strong attractive force between layers. This is in contrast to the silicate mineral montmorillonite, having a low layer charge density, which readily forms an ordered nanocomposite with PAN, accompanied by an increase in basal spacing. This latter composite has been used to form Si–Al non-oxide ceramics under carbothermal reduction conditions [3, 5].

The behaviour of the α-$NbWO_6$ system parallelled that of the Nb_3O_8 system in forming a highly acidic proton form which readily intercalated long-chain amines. The α-$(RNH_3)NbWO_6$ form, although not forming an ordered nanocomposite with PAN, nevertheless underwent reduction to the cubic mixed carbide in its presence. At reaction temperatures greater than 1000 °C, progressive separation of the (Nb, W) carbide into cubic NbC_x and hexagonal WC occurred. The β-$NbWO_6$ system differed in giving a proton form, β-$HNbWO_6$, which appeared unreactive to long-chain amines, possibly due to reduced acidity compared to the α form. Nevertheless, β-$HNbWO_6$ itself underwent carbothermal reduction with PAN, giving a very poorly crystalline cubic carbide (Nb, W)C_x.

Acknowledgements

We thank Mr Hans Jaeger, Mr David Watson and Dr Tim Williams for transmission electron micrographs and selected-area diffraction patterns.

References

1. "Kirk-Othmer Encyclopedia of Chemical Technology", Vol. 4 edited by M. Grayson and D. Ectroth (Wiley Interscience, New York, 1978) pp. 490, 491, 496, 501.
2. Y. SUGAHARA, K. SUGIMOTO, T. YANAGISAWA, Y. NOMIZU, K. KAZUYUKI and C. KATO, *Yogyo Kyokaishi* **95** (1987) 117.
3. Y. SUGAHARA, N. YOKOYAMA, K. KURODA and C. KATO, *Ceram. Int.* **14** (1988) 163.
4. Y. SUGAHARA, K. KURODA and C. KATO, *J. Mater. Sci.* **23** (1988) 3572.
5. T. BASTOW, S. G. HARDIN and T. W. TURNEY, *ibid.* **26** (1991) 1443.

6. M. GASPERIN, *Acta Crystallogr.* **B28** (1982) 2024.
7. W. VIEBAHN, W. RÜDORFF and H. KORNELSON, *Z. Naturforsch.* **22b** (1967) 1218.
8. J. L. FOURQUET, A. LE BAIL and P. A. GILLET, *Mater. Res. Bull.* **23** (1988) 1163.
9. J. BENEKE and G. LAGALY, *Z. Naturforsch.* **33b** (1978) 564.
10. V. BHAT and J. GOPALAKRISHNAN, *J. Solid State Chem.* **63** (1986) 278.
11. R. NEDJAR, M. M. BOREL and B. RAVEAU, *Mater. Res. Bull.* **20** (1985) 1291.
12. V. BHAT and J. GOPALAKRISHNAN, *Solid State Ionics* **26** (1988) 25.
13. R. NEDJAR, M. M. BOREL and B. RAVEAU, *Z. Anorg. Allg. Chem.* **540** (1986) 198.
14. JCPDS-ICDD Powder Diffraction File vers. 2.12 (Swarthmore PA 19081 USA).
15. J. L. FOURQUET, P. A. GILLET and A. LE BAIL, *Mater. Res. Bull.* **23** (1988) 1253.
16. E. K. STORMS, in "Refractory Materials", Vol. 2, edited by J. L. Margrave (Academic Press, New York, 1967) pp. 64 and 65.
17. H. NOWOTNY and R. KIEFFER, *Metallforsch.* **2** (1947) 257.

Received 19 October 1992
and accepted 21 April 1993